Mühendislik Bilimleri ve Tasarım Dergisi
11(2), 631 – 642, 2023
e-ISSN: 1308-6693

Journal of Engineering Sciences and Design
DOI: 10.21923/jesd.1143299

Araştırma Makalesi | Research Article

STABILIZATION OF NOTCHED ELEMENTS' FRACTURE BY USING A CONTROL ALGORITHM

Erol LALE[1*], Bahar AYHAN[1]

[1] İstanbul Technical University, Civil Engineering Faculty, Civil Engineering Department, İstanbul, Türkiye

Keywords

Control Algorithm, Fracture, Finite Element Method, Quasi-brittle, Snap-back.

Abstract

Crack propagation is a significant mechanism for quasi-brittle materials under applied loading. It can occur very suddenly and causes numerical instabilities and deficiencies in some problems. This behavior manifest itself as non-convergence solutions i.e. the inability to obtain the entire load-displacement curve or jumps in the load displacement curve. In this study, a control technique is implemented to obtain the whole load–displacement curve when crack propagation causes severe numerical instabilities such as snap-back behavior. The performance of the control technique was demonstrated by simulating uniaxial tension test of pre-notched plate, three-point bending test of a notched beam and mixed-mode test of a notched plate. This study shows that the control algorithm is able to produce a stable solution path for these kinds of problems. This method can be easily implemented in available commercial finite element codes without the need for any user defined subroutines.

ÇENTİKLİ ELEMANLARIN KIRILMASININ BİR KONTROL ALGORİTMASI KULLANILARAK STABİLİZASYONU

Anahtar Kelimeler

Kontrol Algoritması, Kırılma, Sonlu Elemanlar Yöntemi, Yarı-gevrek, Snap-back (geri tepme).

Öz

Çatlak yayılımı, yük etkisine maruz yarı-gevrek malzemelerin davranışını belirleyen önemli bir mekanizmadır. Çatlak yayılımı çok aniden ortaya çıkabilmekte ve bu da bazı problemlerin analizinde sayısal dengesizliklere ve kusurlara neden olabilmektedir. Bu davranış kendini sayısal sonucun ıraksaması yani bütün yük yerdeğiştirme eğrisinin elde edilememesi olarak veya yük-yerdeğiştirme eğrisinde sıçrama şeklinde gösterir. Bu çalışmada çatlak yayılmasının bütün yük-yer değiştirme eğrisinin elde edilmesinde sayısal sorunlar yarattığı, snap-back (geri tepme) davranışında olduğu gibi, durumlar için bir kontrol algoritması uygulanması verilmiştir. Kontrol tekniğinin performansı tek çentikli levhaya uygulanan doğrudan çekme deneyi, çentikli kirişlerde üç noktalı eğilme deneyi ve iki çentikli levhaların karışık kırılma modu testi simüle edilerek gösterilmiştir. Bu çalışma, kontrol algoritmasının bu tür problemler için kararlı bir çözüm yolu üretebildiğini göstermiştir. Bu yöntem herhangi bir kullanıcı tanımlı alt rutine ihtiyaç duymadan mevcut ticari sonlu eleman kodlarında kolayca uygulanabilir.

Alıntı / Cite

Lale, E., Ayhan, B., (2023). Stabilization of Notched Elements' Fracture by Using a Control Algorithm, Journal of Engineering Sciences and Design, 11(2), 631-642.

Yazar Kimliği / Author ID (ORCID Number)
E. Lale, 0000-0003-4895-5239
B. Ayhan, 0000-0001-9809-097X

Makale Süreci / Article Process	
Başvuru Tarihi / Submission Date	12.07.2022
Revizyon Tarihi / Revision Date	23.01.2023
Kabul Tarihi / Accepted Date	24.02.2023
Yayım Tarihi / Published Date	28.06.2023

* İlgili yazar / Corresponding author: lale@itu.edu.tr, +90-212-285-3752

STABILIZATION OF NOTCHED ELEMENTS' FRACTURE BY USING A CONTROL ALGORITHM

Erol Lale[1†], Bahar Ayhan[1],
[1] İstanbul Technical University, Civil Engineering Faculty, Civil Engineering Department, İstanbul, Türkiye

Highlights

- Implementation of a control technique is introduced to increase loading in a more controlled manner.
- Snap-back behavior is obtained successfully by using proposed control algorithm.
- Simulation of uniaxial tension test of pre-notched plate, three-point bending test of a notched beam and mixed-mode test of a notched plate are conducted to demonstrate the performance of the proposed algorithm.

Graphical Abstract

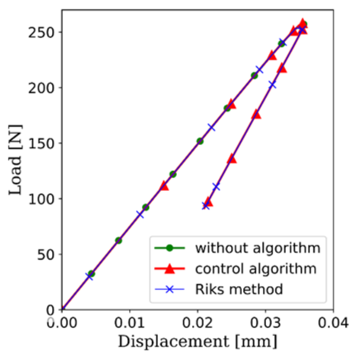

Figure. Load versus crack tip vertical displacement.

Purpose and Scope

The aim of this research is to implement a control technique, which is able to produce a stable solution path, when crack propagation causes severe numerical instabilities such as snap-back behavior.

Design/methodology/approach

A strategy for solving snap-back behavior is developed by introducing auxiliary nodes in order to control load increment. Spring elements are created, which connect the nodes of specimen to auxiliary nodes. Relation between the force of the control node and the displacement of node at the crack is described by arranging stiffness matrix.

Findings

The performance of the control algorithm shows that the relevant control algorithm prevents numerical instabilities and provides a framework which enables increasing load in a more controlled manner.

Research limitations/implications

For future research, it is suggested that same approach can be extended to work under explicit dynamic framework and modified for non-monotonic loading pattern.

Practical implications

It can be easily applied by user who need to stabilize computational models of brittle and quasi-brittle materials fracture. It can reduce computational cost of their research.

Social Implications

There won' t be an impact on society of this research.

Originality

Proposed control algorithm is used to simulate different type of crack propagation problems and results are compared with experimental ones. Researchers who are interested in finite element analysis to simulate failure analysis and crack propagation which shows some numerical stabilities can use this model.

† Corresponding author: lale@itu.edu.tr, +90-212-285-3752

1. Introduction

Quasi-brittle materials have a heterogeneous characteristic which is very significant in many engineering applications. Even under comparatively low load ratios, microcracks initiate and with the increase of load they propagate and grow and some of them may coalesce into macrocracks. This often causes material degradation and affects the performance of the structure. According to the experimental studies, strain localization is observed in the post-peak phase of loading process, which manifests itself as a softening part in load-displacement curve. For quasi-brittle materials, this softening part can be very sharp which arises severe difficulties when simulating it numerically. Therefore, failure study of quasi-brittle materials is of great importance in computational mechanics. Stiffness degradation and strength reduction take place during the softening regime of quasi-brittle materials. It is well known that post-peak behavior cannot be obtained by using load-controlled scheme. On the other hand, if softening part is not too sharp, softening part of the load-displacement curves can be obtained by employing displacement-controlled scheme successfully. In contrast, in some structural problems a sudden decrease in both load and displacement can be observed, as depicted in Figure 1, which is so called snap-back instability. Conventional displacement-controlled scheme cannot find a stable solution for this kind of problem. After the stress attains to its maximum value, the simulations cannot converge and consequently are interrupted.

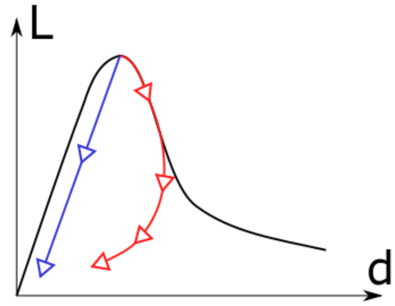

Figure 1. Schematic representation of snap-back behavior

A variety of sophisticated solution techniques have been proposed over decades in order to get an equilibrium state for these kind of problems. A pioneering procedure of solution named as "arc-length" type approach that uses the length of the equilibrium path as a control parameter has been developed independently by Riks (Riks, 1972; Riks, 1979). Wempner (Wempner, 1971), and Ramm (Ramm, 1981). Crisfield (Crisfield, 1981; Crisfield, 1983) modified this mentioned method considering an improved suitability for finite element analysis. Also, Borst (De Borst, 1988; De Borst, 1989) applied a numerical approach, which is an incremental-iterative combination in loading procedure with an indirect displacement control for soil. Moreover, Tvergaard (Tvergaard, 1976) developed a method by defining additional equations in order to provide controlled increase of deformation based on Rayleigh-Ritz method. Instead of pressure, loading is prescribed by increasing the enclosed volume of the domain and it is applied to simulate the stability of internally pressurized elasto-plastic spherical shells. On the other hand, Seguardo and Llorca (Segurado & LLorca, 2004) suggested a different strategy for solving snap-back behavior by introducing an auxiliary node in order to control load increment. This method is based on searching a new variable which monotonically increases during whole loading stage. In their work, they prescribe the sum of crack opening inside a volume while keeping the remote load as a variable of that opening. Paneda et al. followed same approach and employed this approach to get stable result for cohesive crack model (CCM) (Martínez-Pañeda & Fleck, 2018; Martínez-Pañeda, et al., 2017) . In the studies of Carpinteri et al. (Carpinteri, 1989; Carpinteri, 1989; Carpinteri & Colombo, 1989), a cohesive crack model (CCM) is applied in order to investigate the instability problems in softening materials due to size effect, which causes a significant change in the load-displacement curve where crack propagation arises with a sudden drop in the load carrying capacity. Also, Biolzi et al. (Biolzi, et al., 1989; Biolzi, 1990) discovered that large-sized beams exhibited an unstable post-peak behavior and solved this problem with a brittleness number approach. Bocca et al. (Bocca, et al., 1990) used a stress-based assumption to mode-I and mixed mode problems.

Additionally, some numerical simulations require adaptive load-increment (reduction of load increment) beyond post-peak in order to get softening branch encountered while simulating three-point bending test. Especially for the analysis of bigger specimen without notch or specimen with a significantly smaller notch in comparison to the its size (Ayhan, et al., 2021; Lale & Gianluca, 2021). For these kind of difficulties, corresponding control algorithm can be used in order to have more control on crack-mouth opening versus load relation. On the other hand, some simulations might require imposing of constant ratio of displacement in two directions such as mix-mode failure test. For this type of task, control algorithm can offer a great advantage.

The motivation of this paper is to implement a control algorithm by following Seguardo and Llorca (Segurado &

LLorca, 2004) approach, which overcomes the mechanical instabilities as well as enables to increase control over loading pattern. Some numerical examples, such as uniaxial tension test, three-point bending and mixed-mode fracture are simulated in order to investigate the performance of this control algorithm. The numerical results obtained from this study show that relevant control technique makes the loading more controlled and can successfully simulate the snap-back behavior. The presented method will contribute to the development of numerical simulation of the fracture behavior of quasi-brittle materials. It can also improve our understanding of the fracture mechanics of cementitious composites by producing the entire load-displacement correctly, including post-peak.

2. Implementation of Control Algorithm

Here, to describe the algorithm, a simple structural element with a predefined crack having a length of "a" is shown in Figure 2. A plate subjected to a vertical displacement u_y from both sides is considered so that mode-I crack can be observed. An auxiliary node (N_C) is defined as a control node. Also, a node at the crack mouth (N_1) and another node (N_L) on the outer boundary where the loading is applied are described. It is important to mention here that displacement of the crack tip is related to the vertical force of the control node by $u_y^{N_1} = f_y^{N_C}$. Similarly, the displacement of the auxiliary node is taken equal to the vertical force imposed on outer boundary, $u_y^{N_C} = f_y^{N_L}$. Schematic representation of the method to establish these relationships as seen in Figure 2. Two auxiliary spring elements are created, which connect the control node (N_C) with the nodes (N_1) and (N_L), respectively.

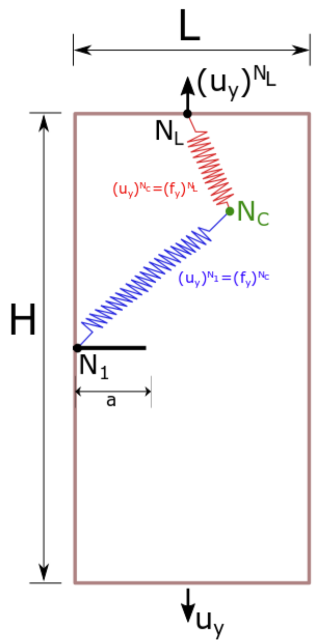

Figure 2. Control algorithm scheme

Relation between the vertical force of the control node and the vertical displacement of node at the crack mouth can be described by using a stiffness matrix as follows;

$$\begin{bmatrix} f_y^{N_1} \\ f_y^{N_C} \end{bmatrix} = \begin{bmatrix} 0 & 0 \\ 1 & 0 \end{bmatrix} \begin{Bmatrix} u_y^{N_1} \\ u_y^{N_C} \end{Bmatrix} \tag{1}$$

On the other hand, second relation between the vertical load of the node on the outer boundary and vertical displacement of the control node is settled with the stiffness matrix below;

$$\begin{bmatrix} f_y^{N_L} \\ f_y^{N_C} \end{bmatrix} = \begin{bmatrix} 0 & 1 \\ 0 & 0 \end{bmatrix} \begin{Bmatrix} u_y^{N_L} \\ u_y^{N_C} \end{Bmatrix} \tag{2}$$

It is worth indicating here that a vertical force should be imposed on the control node in order to provide monotonically increasing vertical crack tip displacement. Moreover, the remote displacement on the outer boundary becomes an outcome of the solution. It should be worth mentioning here that diagonal terms of the stiffness matrices are taken as very small number such as in numerical analysis.

The control algorithm explained in the previous section is implemented via input file of finite element analysis programming software Abaqus (Abaqus, 2011) by providing stiffness matrices, which are defined in Equations (1) and (2). It is important to clarify that the equations explained above are defined for this elementary case. For other types of problems, the stiffness matrices should be redefined due to the crack opening directions.

3. Material Model

Compressive and tensile behavior of concrete are described by using concrete damaged plasticity model (CDPM) of Abaqus, which can represent the behavior of quasi-brittle material. It is based on coupling isotropic damage and plasticity. Typical tensile and compressive stress-strain behavior of the model under uniaxial loading are given in Figure 3.

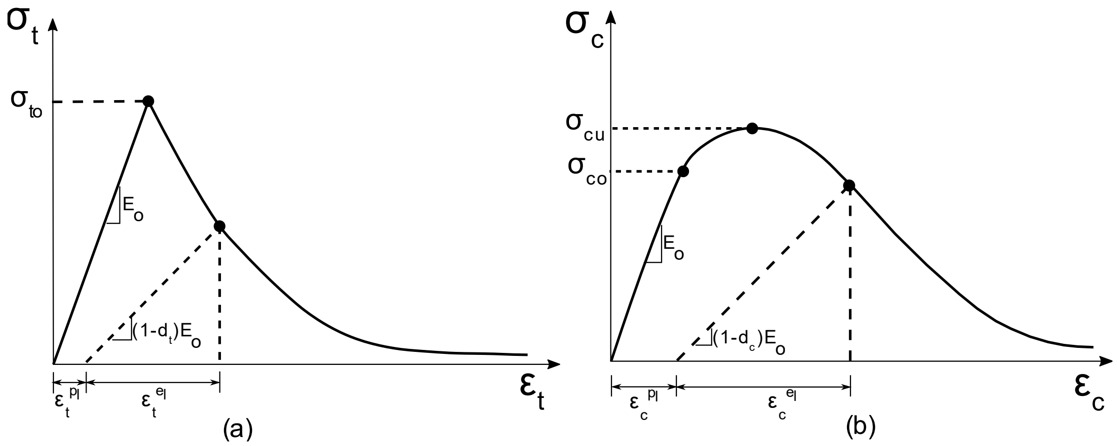

Figure 3. Uniaxial strss-strain behevior of concrete in tension (a) and compression (b), taken from (Abaqus, 2011)

CDPM uses two damage variables; one for tension, d_t, and one for compression, d_c, in order to denote the elastic stiffness decrease, under tension and compression separately. Damage variables can be between zero (intact state) and one (state for fully damage).

$$d_{t,c} = d_{t,c}\left(\varepsilon_{t,c}^{pl}\right); 0 \le d_{t,c} \le 1 \tag{3}$$

where indices *t* and *c* indicate tensile and compressive features. $\varepsilon_t^{pl}, \varepsilon_c^{pl}$ are the effective plastic strains for tensile and compressive strength, which control the evolution of yield surface.

With these two damage variables, stress can be related to strain under uniaxial tension and compression as follow;

$$\sigma_{t,c} = (1-d_{t,c})E_o\left(\varepsilon_{t,c} - \varepsilon_{t,c}^{pl}\right) \tag{4}$$

where E_0 is the intact elastic stiffness of the material.
Under multiaxial loading, stress tensor ($\boldsymbol{\sigma}$) can be desribed as,

$$\begin{aligned} \boldsymbol{\sigma} &= (1-d)\bar{\boldsymbol{\sigma}} \\ \bar{\boldsymbol{\sigma}} &= \mathbf{D}_o^{el} : \left(\boldsymbol{\varepsilon} - \boldsymbol{\varepsilon}^{pl}\right) \end{aligned} \tag{5}$$

Here, $\bar{\boldsymbol{\sigma}}$ denotes effective stress and $\mathbf{D}_o^{el}$ is the elasticity matrix for intact material, *d* stands for damage in multiaxial loadings $d = (1-d_t)(1-d_c)$.

CDPM utilizes following yield surface (F) in effective stress space (Lubliner, et al., 1989; Lee & Fenves, 1998), which enables different evolution of yield surface under tension and compression;

$$F = (1/1-\alpha)\left(\bar{q} - 3\alpha\bar{p} + \beta\left(\varepsilon^{pl}\right)\left\langle\bar{\sigma}_{\max}\right\rangle - \gamma\left\langle-\bar{\sigma}_{\max}\right\rangle\right) - \bar{\sigma}_c\left(\varepsilon_c^{pl}\right) = 0 \quad (6)$$

Here, $\bar{\sigma}_{\max}$ demonstrates principal stress in effective stress space. $\bar{p}$ and $\bar{q}$ denote first and second stress invariants as follows;

$$\bar{p} = -\frac{1}{3}trace(\bar{\sigma}), \quad \bar{q} = \sqrt{\frac{3}{2}(\bar{s}:\bar{s})} \quad (7)$$

Additionally, other parameters required for the definition of yield surface are given below

$$\alpha = \frac{(\sigma_{b0}/\sigma_{c0})-1}{2(\sigma_{b0}/\sigma_{c0})-1}; 0 \le \alpha \le 0.5$$
$$\beta = \frac{\bar{\sigma}_c\left(\varepsilon_c^{pl}\right)}{\bar{\sigma}_t\left(\varepsilon_t^{pl}\right)}(1-\alpha)-(1+\alpha) \quad (7)$$
$$\gamma = \frac{3(1-K_c)}{2K_c-1}$$

Here, $\psi, \sigma_{to}, \varsigma$ denote the dilatation angle, the uniaxial tensile strength and eccentricity parameter, respectively.

4. Numerical Simulation

In this section, numerical examples are conducted to demonstrate the performance of control algorithm. These examples include Mode-I and mixed mode fracture (Mode-I+Mode-II) propagation. Moreover, an example to overcome the snap-back instability is also presented.

4.1. Uniaxial Tension Specimen

Uniaxial tension specimen (UTS) is modeled to simulate mode-I fracture. All geometrical details and boundary conditions are depicted in Figure 4. Specimen is assumed under plane strain condition by preventing the out-of-plane deformation. A concentrated force is imposed in the vertical direction on the control node $f_y^{N_C} = 0.05$. In the simulation, CDPM is used to define material property of the specimen. Young's modulus and Poisson's ratio are chosen as E=30GPa and ν=0.2, respectively. Tensile behavior is defined by using tensile strength and the fracture energy, f_t=3MPa and G_f=20Joule/m^2.

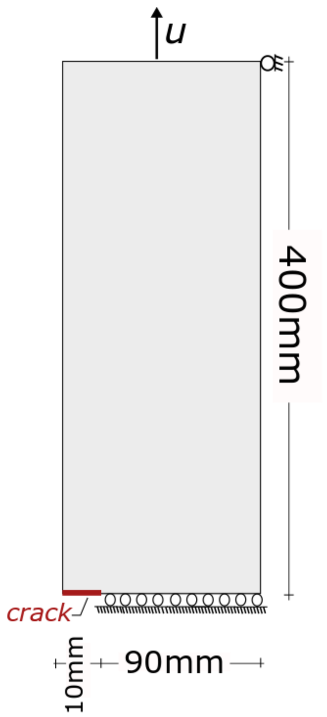

Figure 3. Geometrical details of uniaxial tension specimen (UTS)

The specimen is analyzed for 3 cases; first case is without control algorithm, second one is with control algorithm and last one is with the solution using Riks method (arc-length method) developed previously in the works of Riks (Riks, 1972; Riks, 1979). Obtained load-displacement curves are shown in the Figure 5. It can be seen from the figure that the model without control algorithm can only reaches the peak point and cannot go on beyond peak and analysis is interrupted, which means it cannot capture snap-back behavior. However, it is worth noting that model with control algorithm can capture snap-back behavior like Riks method.

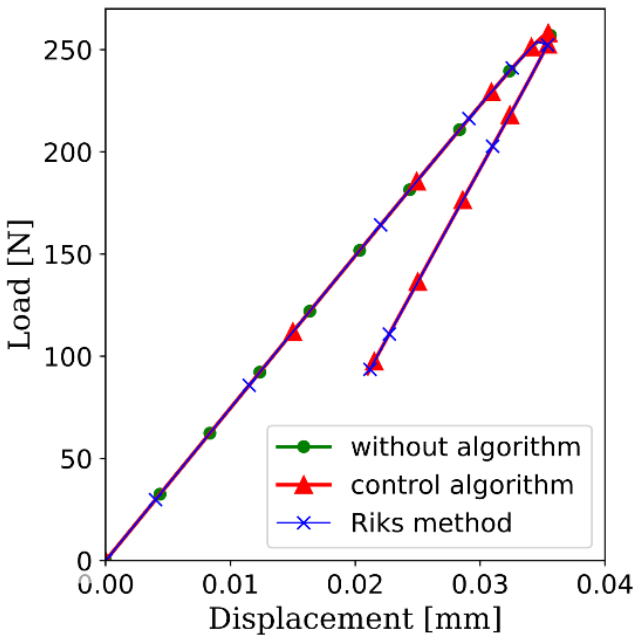

Figure 5. Load versus crack tip vertical displacement

4.2. Three-point Bending Beam Test

Three-point bending beam with a predefined notch which is also an example of Mode-I failure is simulated to investigate load versus crack mouth opening displacement (CMOD) behavior. Geometrical and loading details of the specimen, which are taken from the experimental study performed by Hoover et al. (Hoover, et al., 2013), are presented in Figure 6a. The thickness of the beam is t=40mm. Control algorithm implemented in the input file is defined using the tip nodes (N_1 and N_2) at the two sides of the notch, as shown in Figure 6b. Control node (N_C) is connected to these two tip nodes with two linear elements and to a remote boundary node (N_L) with one linear element.

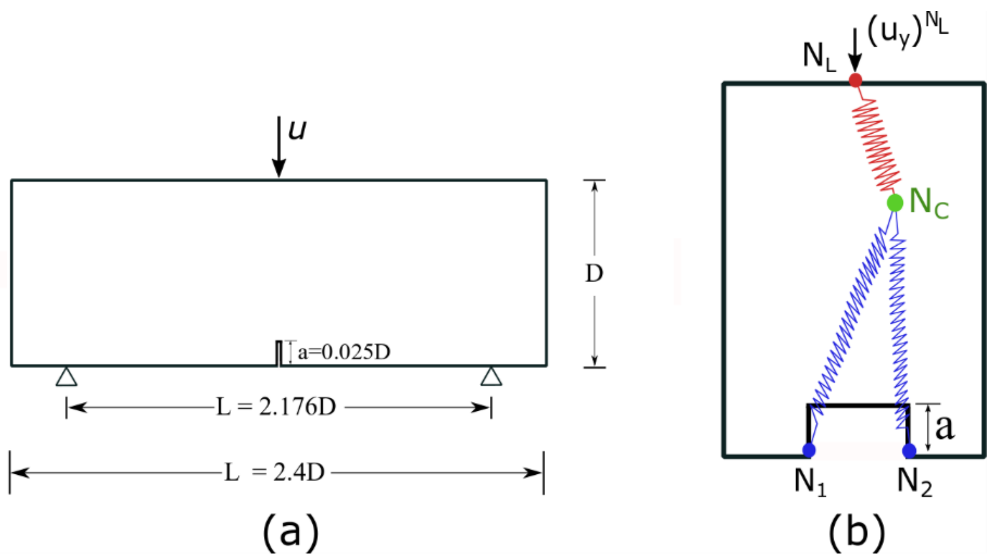

Figure 6.a) Geometrical details of three-point bending specimen b) control algorithm scheme.

Here, horizontal displacements of the crack tip nodes are utilized to calculate CMOD, as $\left(u_x^{N_1} - u_x^{N_2}\right)$. The relation between the crack mouth nodes and control node is given by a stiffness matrix as follows;

$$\begin{bmatrix} 0 \\ 0 \\ 0 \\ 0 \\ f_x^{N_C} \\ f_y^{N_C} \end{bmatrix} = \begin{bmatrix} 0 & 0 & 0 & 0 & 0 & 0 \\ 0 & 0 & 0 & 0 & 0 & 0 \\ 0 & 0 & 0 & 0 & 0 & 0 \\ 0 & 0 & 0 & 0 & 0 & 0 \\ 0 & 0 & 0 & 0 & 0 & 0 \\ 1 & 0 & -1 & 0 & 0 & 0 \end{bmatrix} \begin{Bmatrix} u_x^{N_1} \\ u_y^{N_1} \\ u_x^{N_2} \\ u_y^{N_2} \\ u_x^{N_C} \\ u_y^{N_C} \end{Bmatrix} \tag{10}$$

In this example, an element with two degree-of-freedom $\left(u_x, u_y\right)$ is required in order to describe CMOD as a function of vertical force applied on the control node. Also, the relation between control node and remote node (Loading one) is similar as described in Equation (2).

In the simulation, material properties of the quasi-brittle specimen are selected as follows; modulus of elasticity is E=30GPa, Poisson's ratio is ν=0.2. Tension softening part of the material is characterized with a tensile stress of f_t=3MPa and a fracture energy of G_f=20Joule/m^2. The vertical concentrated force is subjected to control node NC to obtain the load versus the opening displacement of crack. Figure 7 shows a comparison between the models with (Imp-cont) and without control (Imp-wo-cont) algorithm as well as experimental results for the beam D=215, 500 mm. From the Figure 7a, it can be seen that for D=215 mm, analysis without control algorithm stops at the peak and cannot find a proper solution path whereas the simulation with control algorithm is able to capture post peak successfully. Also, one can easily notice that while explicit simulation gives an oscillatory post-peak behavior, model with control algorithm produces a smooth post-peak response which is compatible with experimental results. Figure 7b demonstrates results for the beam having depth D=500 mm, simulation under the framework of implicit with control algorithm and explicit analysis give similar results as they produce in D=215 mm. On the other hand, simulation without control algorithm can find a solution path beyond the peak but behavior exhibit a very large jump which doesn't produce correct post-peak behavior as can be seen from the figure. Overall, control algorithm can capture peak values correctly and produce a smooth post-peak behavior.

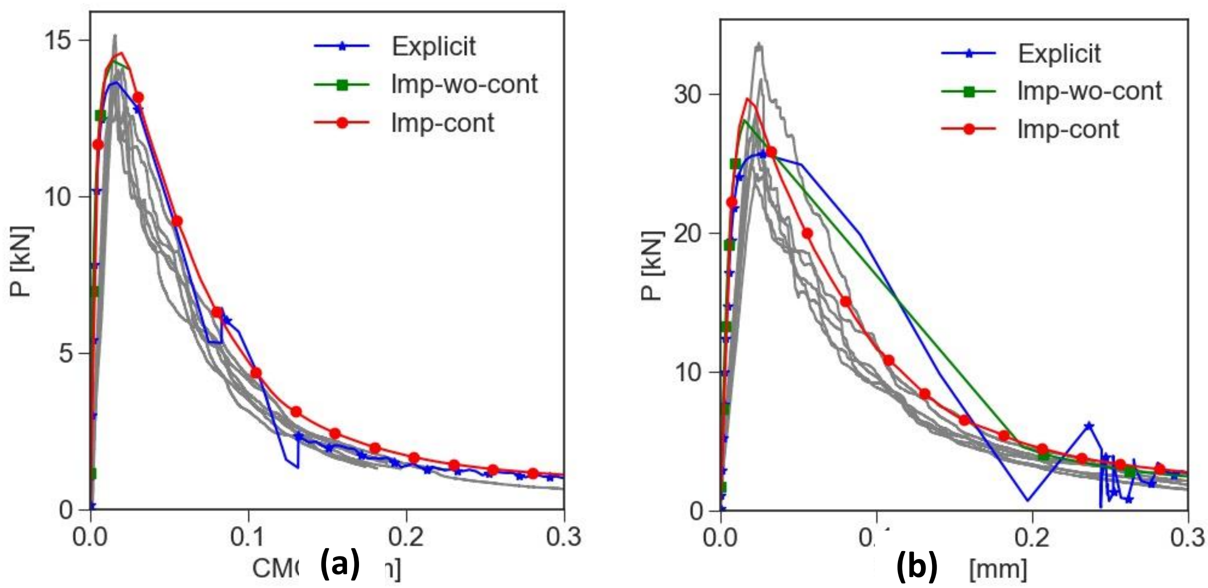

Figure 4. Load versus crack mouth opening displacement (CMOD) curve of three-point bending test; a) D=215 mm, b) D=500 mm.

4.3. Mixed Mode Specimen

Double Edge Notched (DEN) specimen is considered to simulate the mixed mode fracture, which is a combination of Mode-I and Mode-II (Nooru-Mohamed, 1993), where the specimen is subjected to lateral and axial displacements simultaneously. Points where vertical and lateral displacement obtained in the experimental study are shown in Figure 8. Axial deformation δ_N of the specimen is calculated by considering average vertical displacement between N_1N_2 and N_3N_4. On the other hand, lateral deformation δ_S is taken as the average horizontal displacement between S_1 and S_2. In the experimental research, these specimens are subjected to different loading paths like δ_N/δ_S =1 or δ_N/δ_S=2 and so on.
It is worth mentioning here that in the simulation it is not easy to keep loading ratio constant during fracturing process without control algorithm.
The dimensions and boundary conditions of DEN specimen are shown in Figure 8. The mechanical properties of the material are selected as follows; Elasticity modulus is E=30000MPa, Poisson's ratio is ν=0.2. Tensile and compressive stresses are f_t=2.4MPa and f_c=33.6MPa, respectively. It is also noted that while out-of-plane thickness is 50 mm in experimental research, it is taken as 5 mm in order to decrease the computational cost.

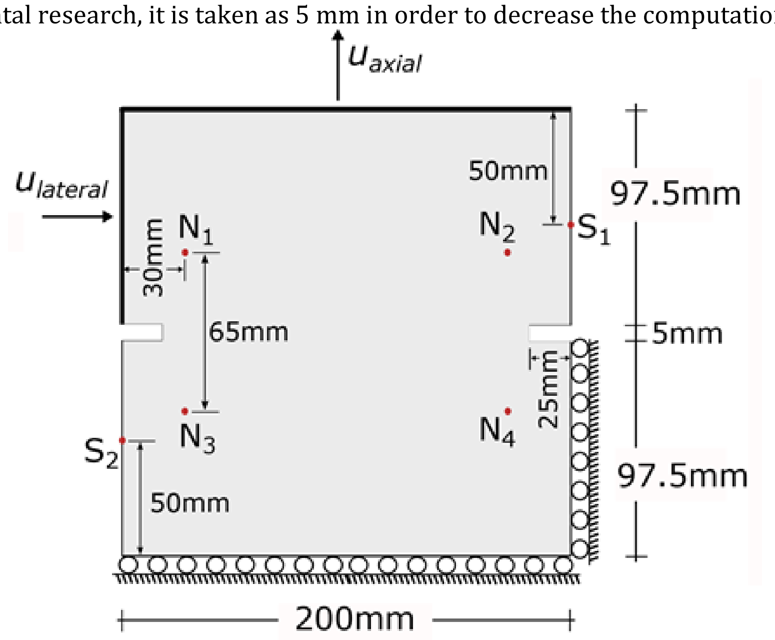

Figure 5. Geometrical details of double edge notched (DEN) specimen (Nooru-Mohamed, 1993)

In order to keep constant ratio between axial and lateral deformation during the loading of the specimen, additional stiffness matrices are defined in the input file of Abaqus. Two control algorithms are implemented separately, for the axial (δ_N) and lateral (δ_S) deformation. The first auxiliary element is defined between a control node and the nodes (N_1, N_2, N_3, N_4) as well as another element between the same control node and a remote node for u_{axial}. Here, vertical displacement of specimen is described in terms of $u_y^{N_1}, u_y^{N_2}, u_y^{N_3}, u_y^{N_4}$, which is assigned as the force of auxiliary control node, $f_y^{N_c} = \left(\dfrac{u_y^{N_1} + u_y^{N_2} - u_y^{N_3} - u_y^{N_4}}{2} \right)$. The relation between the corresponding nodes and control node can be described using following stiffness matrix;

$$\begin{Bmatrix} 0 \\ 0 \\ 0 \\ 0 \\ f_y^{N_C} \end{Bmatrix} = \begin{bmatrix} 0 & 0 & 0 & 0 & 0 \\ 0 & 0 & 0 & 0 & 0 \\ 0 & 0 & 0 & 0 & 0 \\ 0 & 0 & 0 & 0 & 0 \\ 0.5 & 0.5 & -0.5 & -0.5 & 0 \end{bmatrix} \begin{Bmatrix} u_y^{N_1} \\ u_y^{N_2} \\ u_y^{N_3} \\ u_y^{N_4} \\ u_y^{N_C} \end{Bmatrix} \tag{11}$$

The second auxiliary element is prescribed for the lateral deformation. Lateral displacement of the specimen is defined in terms of the lateral displacement at the nodes (S_1, S_2) and another element between the same control node and a remote node on the boundary. Lateral displacement of the specimen is defined by the horizontal displacements at S_1 and S_2 ($u_x^{S_1}, u_x^{S_2}$), and it is taken equal as the horizontal force on the control node (N_c) as

$f_x^{N_c} = \left(u_x^{S_1} - \frac{u_x^{S_2}}{2} \right)$. The relation between the crack tip nodes and control node can be given by a following stiffness matrix;

$$\begin{Bmatrix} 0 \\ 0 \\ f_x^{N_C} \end{Bmatrix} = \begin{bmatrix} 0 & 0 & 0 \\ 0 & 0 & 0 \\ 1 & -0.5 & 0 \end{bmatrix} \begin{Bmatrix} u_x^{S_1} \\ u_x^{S_2} \\ u_x^{N_C} \end{Bmatrix} \tag{12}$$

Same relation between the control node and the node on the upper left part of the specimen are defined as shown in previous examples.

Obtained result for the test loaded equal vertical and lateral displacement is given in Figure 9. During the all phases of the simulation, the ratio between axial and lateral deformation $\delta_N/\delta_S = 1$ is obtained, and given in Figure 9a. Load versus axial and lateral displacements are plotted together with the experimental results, as shown in Figure 9b-c.

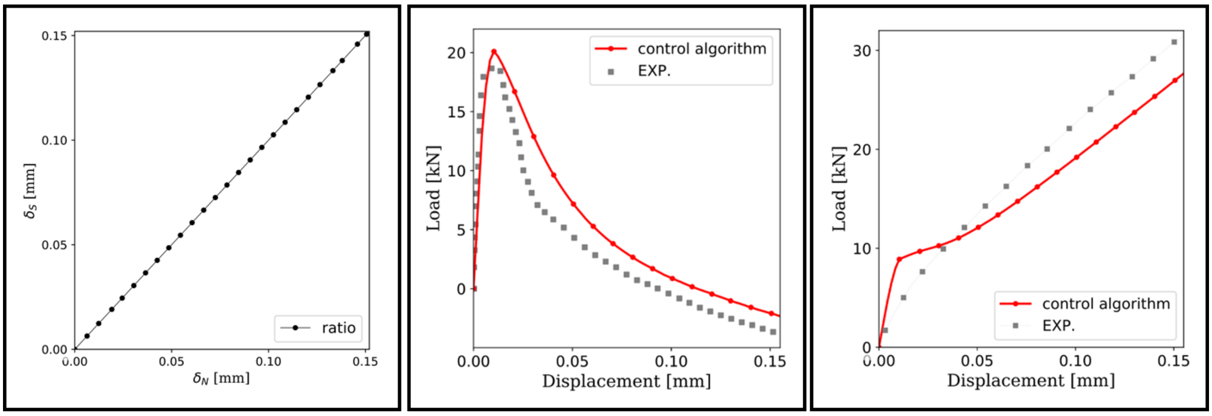

(a) (b) (c)

Figure 6.a) Calculated axial deformation versus lateral deformation $\delta_N/\delta_S = 1$ b) Axial load-displacement curves c) Lateral load-displacement curves.

Similarly, Figure 10 shows the curves of the simulation having loading ratio as $\delta_N/\delta_S = 2$. The ratio between axial and lateral deformation $\delta_N/\delta_S = 2$ is given in Figure 10a. Load versus axial and lateral displacements as well as experimental results are given in Figure 10b-c.

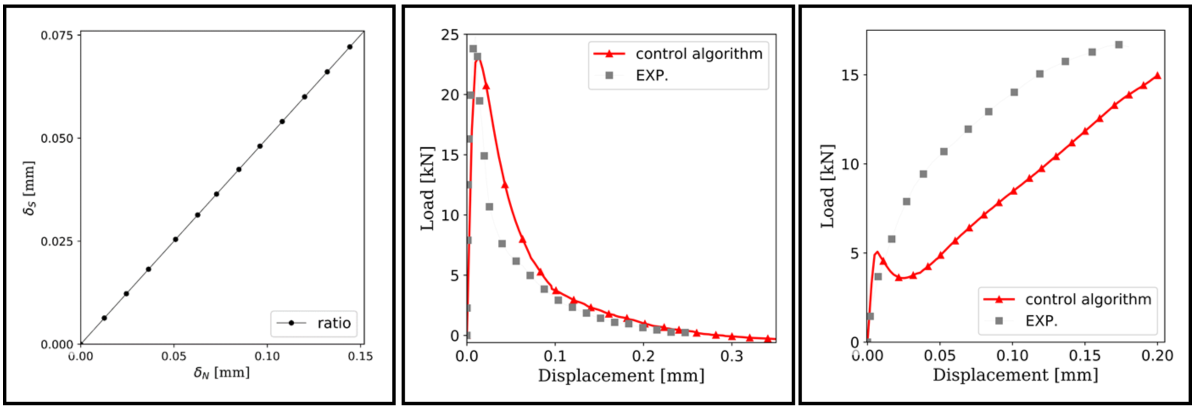

(a) (b) (c)

Figure 10.a) Calculated axial deformation versus lateral deformation $\delta_N/\delta_S = 2$ b) Axial load-displacement curves c) Lateral load-displacement curves.

Models with implemented control algorithm can capture load versus displacement curves for both directions quite well and it enables to control loading ratio successfully.

5. Results

A control algorithm is implemented to increase loading in a more controlled manner and its performance is investigated using three different simulations; one of them uniaxial tension test which exhibit snap-back behavior, the other one is three-point bending beam test and last one is mixed mode test which is to be subjected to constant ratio of displacement in two directions. The performance of the control algorithm in the finite element model is demonstrated that the whole load-displacement curve can be obtained while simulating brittle and quasi-brittle failures. Based on this study, the following conclusions can be drawn

i) The employed control algorithm is able to handle snap-back behavior successfully.
ii) Control algorithm provides a framework which enables increasing load in a more controlled manner such as increasing load on remote nodes result a monotonic increase in crack opening.
iii) When a more sophisticated loading scheme is required, it can be employed as shown in mixed mode simulations.

For the future study, same approach will be extended to work under explicit dynamic framework and it will be modified for non-monotonic loading pattern.

Conflict of Interest

No conflict of interest was declared by the authors.

References

Abaqus. (2011). Providence, RI, USA.: Dassault Systemes Simulia Corporation.

Ayhan, B., Lale, E. & Celik, N., 2021. Size effect analysis of concrete beams under bending using crack-band approach.. *Journal of Polytechnic,* pp. 1-1.

Biolzi, L., 1990. Mixed mode fracture in concrete beams. *Engineering Fracture Mechanics,* 35(1-3), pp. 187-193.

Biolzi, L., Cangiano, S., Tognon, G. & Carpinteri, A., 1989. Snap-back softening instability in high-strength concrete beams.. *Materials and Structures,* 22(6), pp. 429-436.

Bocca, P., Carpinteri, A. & Valente, S., 1990. Size effects in the mixed mode crack propagation: softening and snap-back analysis. *Engineering Fracture Mechanics,* 35(1-3), pp. 159-170.

Carpinteri, A., 1989. Post-peak and post-bifurcation analysis of cohesive crack propagation. *Engineering Fracture Mechanics,* 32(2), pp. 265-278.

Carpinteri, A., 1989. Softening and snap-back instability in cohesive solids. *International Journal for Numerical Methods in Engineering,* 28(7), pp. 1521-1537.

Carpinteri, A. & Colombo, G., 1989. Numerical analysis of catastrophic softening behavior (snap-back instability). *Computers & Structures,* Volume 31, pp. 607-636.

Crisfield, M., 1981. A fast incremental/iterative solution procedure that handles "snap-through". *Computational methods in nonlinear structural and solid mechanics,* pp. 55-62.

Crisfield, M., 1983. An arc-length method including line searches and accelerations. *International journal for numerical methods in engineering,* pp. 1269-1289.

De Borst, R., 1988. Bifurcations in finite element models with a non-associated flow law. *International Journal for Numerical and Analytical Methods in Geomechanics,* 12(1), pp. 99-116.

De Borst, R., 1989. Numerical methods for bifurcation analysis in geomechanics. *Ingenieur-Archiv.,* 59(2), pp. 160-174.

Hoover, C. G. et al., 2013. Comprehensive concrete fracture tests: Description and results. *Engineering Fracture Mechanics,* Volume 114, pp. 92-103.

Lale, E. & Gianluca, C., 2021. Symmetric high order microplane model for damage localization and size effect in quasi-brittle materials. *International Journal for Numerical and Analytical Methods in Geomechanics,* 45(10), pp. 1458-1476.

Lee, J. & Fenves, G. L., 1998. Plastic-Damage Model for Cyclic Loading of Concrete Structures. *Journal of Engineering Mechanics,* Volume 124(8), pp. 892-900.

Lubliner, J., Oliver, J., Oller, S. & Oñate, E., 1989. A Plastic-Damage Model for Concrete. *International Journal of Solids and Structures,* Volume 25, pp. 299-329.

Martínez-Pañeda, E., del Busto, S. & Betegón, C., 2017. Non-local plasticity effects on notch fracture mechanics. *Theoretical and Applied Fracture Mechanics,* Volume 92, pp. 276-287.

Martínez-Pañeda, E. & Fleck, N. A., 2018. Crack growth resistance in metallic alloys: the role of isotropic versus kinematic hardening. *Journal of Applied Mechanics,* 85(11), p. 111002.

Nooru-Mohamed, M. B., 1993. *Mixed-mode fracture of concrete: An experimental approach.* The Netherlands: Delft University of Technology.

Ramm, E., 1981. *Strategies for Tracing the Nonlinear Response Near Limit.* Berlin: Springer.

Riks, E., 1972. The application of Newton's method to the problem of elastic stability.. *Journal of Applied Mechanics.,* pp. 1060-1066.

Riks, E., 1979. An incremental approach to the solution of snapping and buckling problems. *International Journal of Solids and Structures,* pp. 529-551.

Segurado, J. & LLorca, J., 2004. A new three-dimensional interface finite element to simulate fracture in composites. *İnternational Journal of Solids and Stuctures,* 41(11-12), pp. 2977-2993.

Tvergaard, V., 1976. Effect of thickness inhomogeneities in internally pressurized elastic-plastic spherical shells.. *Journal of the Mechanics and Physics of Solids,* 24(5), pp. 291-304.

Wempner, G. A., 1971. Discrete approximations related to non-linear theories of solids. *International Journal of Solids and Structures,* pp. 1581-1599.